Electronic Supplementary Material (ESI) for Nanoscale.

Supporting Information

Heavy doping ceria by wet impregnation: A viable alternative to bulk doping approaches

Mihaela Florea[1], Daniel Avram[2], Adrian Maraloiu[1], Bogdan Cojocaru[3] and Carmen Tiseanu[2, *]

[1]National Institute of Materials Physics, 405A Atomistilor Street, 077125 Magurele-Ilfov, Romania

[2]National Institute for Laser, Plasma and Radiation Physics, P.O. Box MG-36, RO 76900, Bucharest-Magurele, Romania

[3]Department of Organic Chemistry, Biochemistry and Catalysis, University of Bucharest, 4-12 Regina Elisabeta Bvd, Bucharest, 030016, Romania

*Email: carmen.tiseanu@inflpr.ro

Structural characterization and luminescence methods

Powder X-ray diffraction (XRD) patterns were recorded on a Schimadzu XRD - 7000 diffractometer using Cu Kα radiation at a scanning speed of 0.10 degrees min-1 in the 15 ÷ 90 degrees 2Θ range.

X-Ray Photoelectron Spectroscopy (XPS). The XPS measurements were performed in an ESCALAB Xi+ (Thermo SCIENTIFIC Surface Analysis) setup equipped with a multichannel hemispherical electron Analyzer (dual X-ray source) working with Al Kα radiation (hν= 1486.2 eV), using C 1s (284.4 eV) as the energy reference. XPS data were recorded by slightly pressing powered materials that had been outgassed in the pre-chamber of the instrument at room temperature at a pressure of <2 × 10−8 Torr to remove chemisorbed water from their surfaces. The surface chemical compositions and oxidation states were estimated from the XPS spectra by calculating the integral of each peak after subtraction of the "S-shaped" Shirley-type background using the appropriate experimental sensitivity factors by means of Avantage software (version 5.978).

Microbeam X-ray fluorescence (micro-XRF) spectrometry was performed on a custom-made instrument with an X-ray tube: Oxford Instruments, Apogee 5011, Mo target, focus spot ~40 µm, max. high voltage - 50 kV, max current - 1 mA, Amptek X-123 complete X-Ray spectrometer with Si - PIN detector. The key element of the micro - XRF instrument is an X-ray policapillary minilens (IfG-Institute for Scientific Instruments) which provides a focal spot size on the sample of 15 - 20 micrometers.[S1]

Raman analysis was carried out with a Horiba Jobin Yvon - Labram HR UV-Visible-NIR Raman Microscope Spectrometer at 514 nm. (1 mm spot size, 1.5 microns confocal resolution along optical axis, 0.5 microns lateral spatial resolution, 0.7 cm^{-1} spectral resolution)

*Scanning Electron Microscopy with Energy Dispersive Spectra (SEM-EDS)*were acquired by use of an FEI Inspect S Electron Scanning Microscope equipped with EDAX Si(Li) detector.

Transmission Electron Microscopy (TEM) observations were done using JEOL 2100 microscope operated at 200 kV and equipped with a JEOL JED-2300T unit for Energy-Dispersive X-Ray spectroscopy (EDS) analysis. EDS mapping in Scanning Transmission Electron Microscopy (STEM) mode was performed to determine the distribution of the component elements in the ceria samples. The powder samples were crushed in a mortar, diluted with ethanol and sonicated for 3 min. Then a drop of the sample was let to dry on a standard 400 mesh copper grid with lacey carbon film. Areas of Yb(I), Tm- CeO_2 and Yb(B), Tm- CeO_2, calcined at 300 °C and 1000 °C (Figure 3) were scanned with a convergent beam of aprox. 0.5 nm diameter and the X-ray signal from each point of the scan arrived at the detector. Using K lines for O and L lines for Ce and Yb, the maps of selected elements were obtained after 120 sweeps.

Diffuse reflectance (DR-UV/NIR) spectra were recorded using a UV3600 UV-VIS Shimadzu spectrophotometer equipped with Shimadzu ISR-3100 Integrating Sphere Attachment and two light sources - D_2 (deuterium) lamp for the ultraviolet range WI (halogen) lamp for the visible and near-infrared range. The spectra were recorded in the range of 220–2600 nm with a wavelength step of 2 nm, working with a slit width of 8 nm (for 220–800 nm) and 32 nm (for 800–2600 nm). The UV-VIS spectra were measured using samples diluted with extra pure barium sulphate (purchased from Nacalai Tesque).

The Brunauer-Emmett-Teller (BET) method was used to calculate the specific surface area from the data obtained at P/P_0 between 0.01 and 0.995 using a Micrometrics instrument (ASAP 2010). Prior to surface area determination, all powders were degassed at 150 °C for 5h.

Luminescence measurements. Luminescence spectra were recorded at room temperature using a wavelength tunable NT340 Series EKSPLA OPO (Optical Parametric Oscillator) with laser spectral width around 5 cm^{-1}, operated at 10 Hz. For cw up-conversion measurements, a fiber coupled laser diode centered at 975 nm was used (RLTMFC-980-4W-5). Around 980 nm, the energy per pulse was 7 mJ with an average power density of 2.23 W/cm^2 . As detection system, an intensified CCD (iCCD) camera (Andor Technology, iStar iCCD DH720) coupled to a spectrograph (Shamrock 303i, Andor) was used.To avoid the emission laser line from the fiber coupled laser to temper with the iCCD detector, a bandpass filter at 970 nm (10 nm bandpass) was used. For the digital photos registered in up-conversion measurements, a Canon EOS 60D camera with 5 s integration time and 1000 ISO was used. For the comparison of the up-conversion emission intensity, the laser power density was kept constant to 2.23 W/cm^2. The powder samples were placed in the same geometrical configuration on a solid sample holder (sample holder area of 14 mm X 7 mm, from Horiba Scientific, J1933) in reflection mode. The laser was focused on a 2.5 mm spot and a premium hard-coated edge pass filter (FESH0900, Thorlabs) was used to protect the detection system from the incident laser. The up-conversion emission spectra were recorded using the same parameters: delay after the laser pulse of 0.1 µs, gate width of 100 µs, gain level of the iCCD was set to 150 and the input slit was set to 50 µm. A grating with 150 l/mm groove density and 800 nm blaze was used. The integration window of the iCCD was centered at 670 nm to cover the emission spectra of Tm from 450 to 850 nm. The Eu luminescence measurements were carried out using a Fluoromax 4 spectrofluorometer (Horiba). The luminescence decays were measured by using the "decay by delay" feature of the phosphorescence mode.

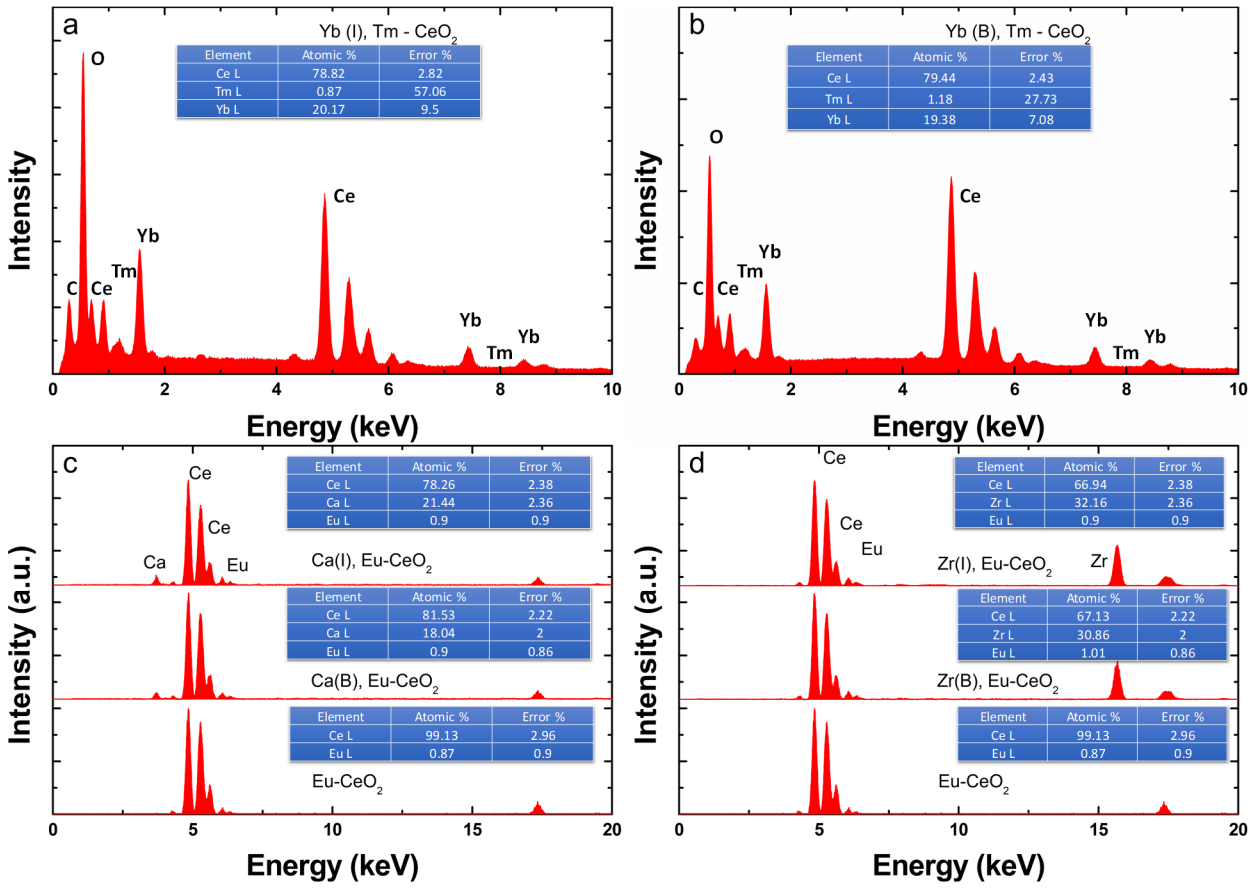

Figure S1. The energy dispersive spectroscopy (EDX-SEM spectra of ((a) Yb (I), Tm – CeO_2 and (b) Yb (B), Tm – CeO_2 calcined at 300 °C. The inset tables contain the corresponding atomic ratio/ weight ratio of the detected elements and their corresponding error. The atomic contents of Yb and Tm are estimated around 19-21 and 0.8-1.2% in good agreement with concentration measured on cationic precursors. XRF spectra (c,d) confirmed also similar metal content and dopant (Eu, Ca, and Zr) concentration in both impregnated and bulk doped samples, close to the nominal concentration of 1% (Eu), 20% (Ca) and 30% (Zr).

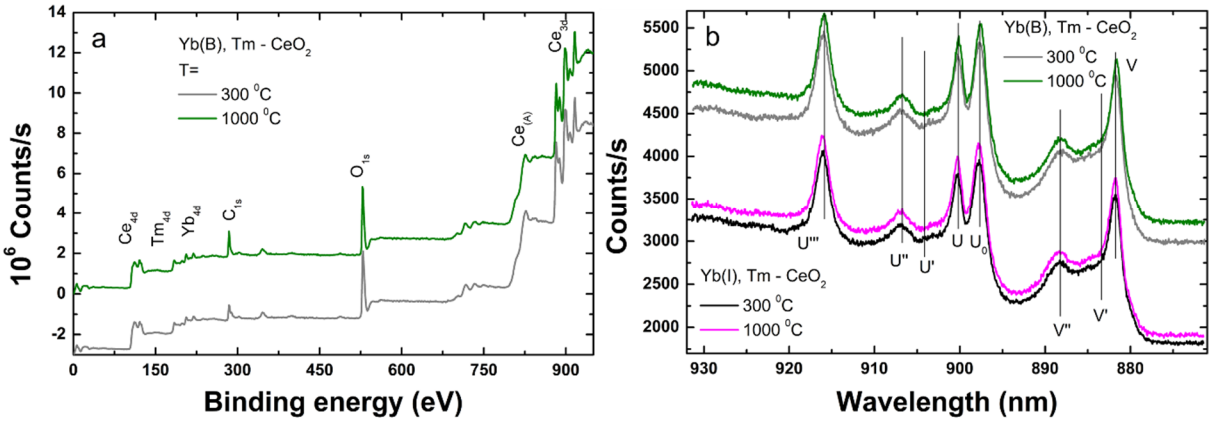

Figure S2. (a)XPS survey of Yb(B), Tm- CeO_2 - 300°C and Yb(B), Tm- CeO_2 - 1000° C. (b) XPS Ce3d spectra of Yb(B), Tm- CeO_2 and Yb(I), Tm- CeO_2calcined at 300 and 1000° C.

In agreement with literature [S2-S4], the decomposition of the Ce 3d spectrum yields five spin-orbit split doublets denoted as v_0/u_0, v/u, v'/u', v''/u'', v'''/ u''' (**Figure S2b**). The doublets v_0/u_0 and v'/u' are related to Ce in the +3 oxidation state while the others are due to Ce^{4+} ions. In all samples analyzed samples, Ce is present in both oxidation states, irrespective of Yb doping mode and anneal temperature.

Tabel S1. Atomic fractions of Ce ions in the +3 oxidation state and surface Ce/ Yb atomic ratio as a function of Yb insertion mode (bulk doping versus wet impregnation) and anneal temperature

Sample	**[Ce] / [Ce]+[Yb] (%)**		**[Ce^{3+}] / [Ce^{3+}]+[Ce^{4+}] (%)**	
	300°C	1000°C	300°C	1000°C
Yb (B), Tm -CeO_2	81.35	81.74	44.74	29.20
Yb (I), Tm-CeO_2	81.35	81.63	49.35	28.72

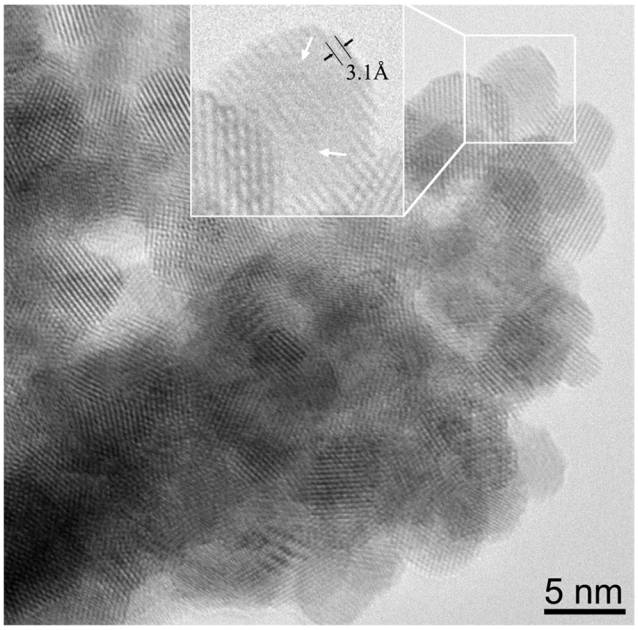

Figure S3. HRTEM image of Yb(I), Tm- CeO_2 calcined at 300 °C showing crystallized particles with lattice spacing of 3.1 Å corresponding for (111) planes of cubic CeO_2 but also the presence of some amorphous regions (indicated by white arrows).

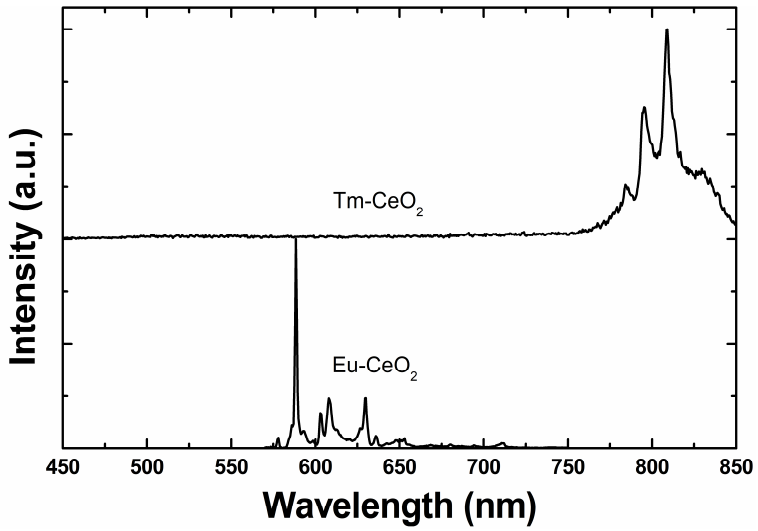

Figure S4. The emission spectra of the as –synthetized Tm-CeO_2 and Eu-CeO_2 used as supports for impregnation under excitation into O^{2-}- Ce^{4+} charge transfer band of CeO_2 (at ~355 nm). The narrow shaped spectra as well as the emission sensitization *via* the charge-transfer of CeO_2 confirm that Tm or Eu substitute for the Ce(4+) lattice sites prior to anneal.

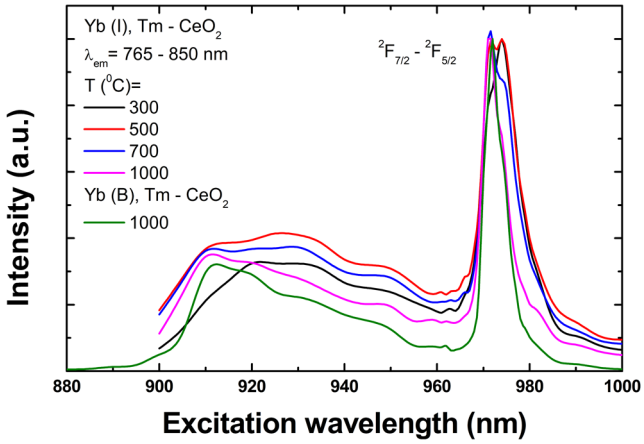

Figure S5. Evolution of the up-conversion excitation spectra of impregnated ceria with anneal temperature monitoring the strongest emission at 800 nm.

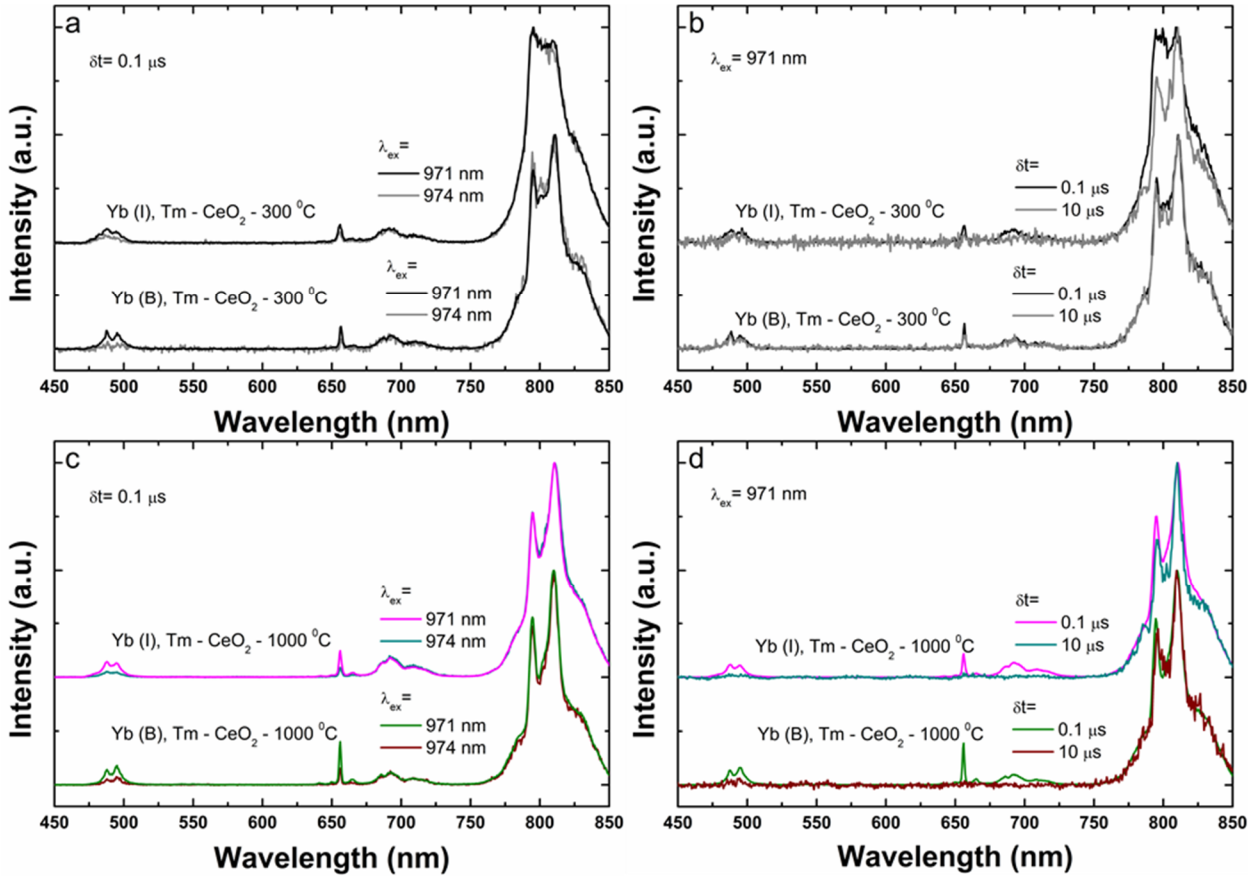

Figure S6. Using both spectral (a, c) and temporal (b, d) selectivity, the up-conversion emission spectra of impregnated and bulk doped ceria samples show slightly different emissions shapes around 800 nm at low anneal temperature (300 °C).

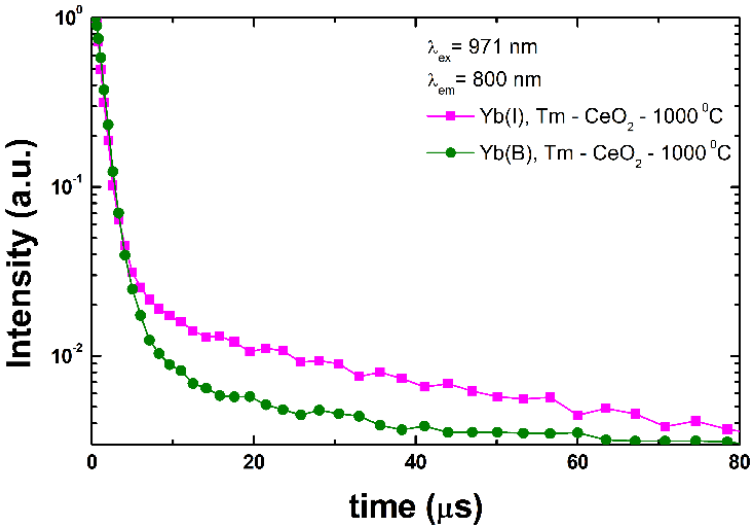

Figure S7. Comparison between the up-conversion emission decays of Tm in impregnated and bulk doped ceria (emission excited at 971 nm and monitored at 800 nm).

As shown in the previous **Figure S6**, scanning the excitation profiles revealed at least two excitation wavelengths at 971 and 974 nm that deliver slightly different UPC emission shapes. When the temporal resolution (that is, delay after the laser pulse) is added, different up-conversion emission shapes around strongest Tm emission at 800 nm could be separated as a result of their distinct dynamics.

Figure S7 shows that the up-conversion emission decays of impregnated and bulk doped ceria calcined at 1000 °C differ only in the long tail decay time. The effect may originate from Tm with fewer Yb (and associated vacancy defects) in their neighbourhood and thus less subjected to back transfer from Tm to Yb or/and deleterious cross-relaxation processes due to inhomogeneous doping . [S5]

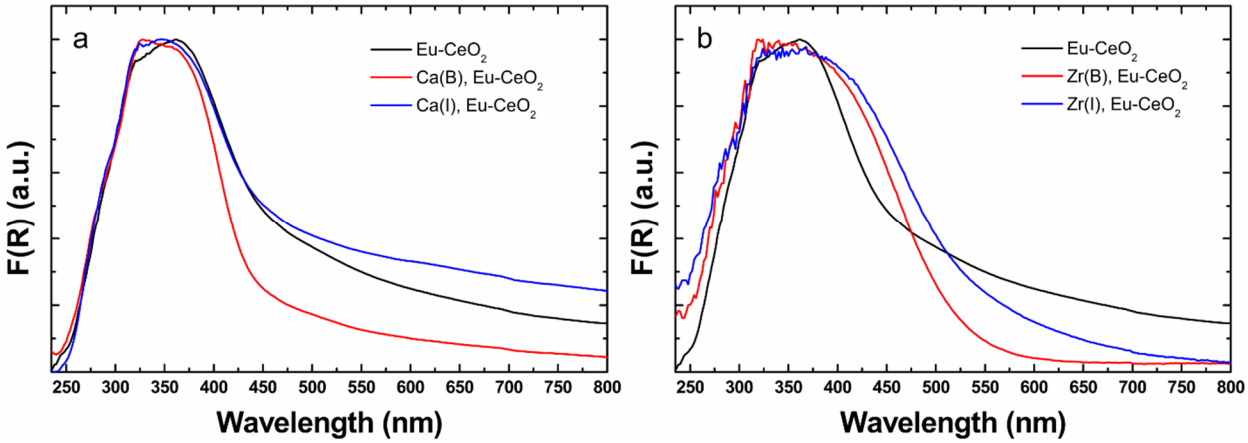

Figure S8. Diffuse reflectance spectra of Ca (a) and Zr (b) impregnated and bulked doped CeO_2. No absorption band characteristic of tetragonal ZrO_2 (around 240 nm) can be observed for Zr impregnated or bulk doped ceria.

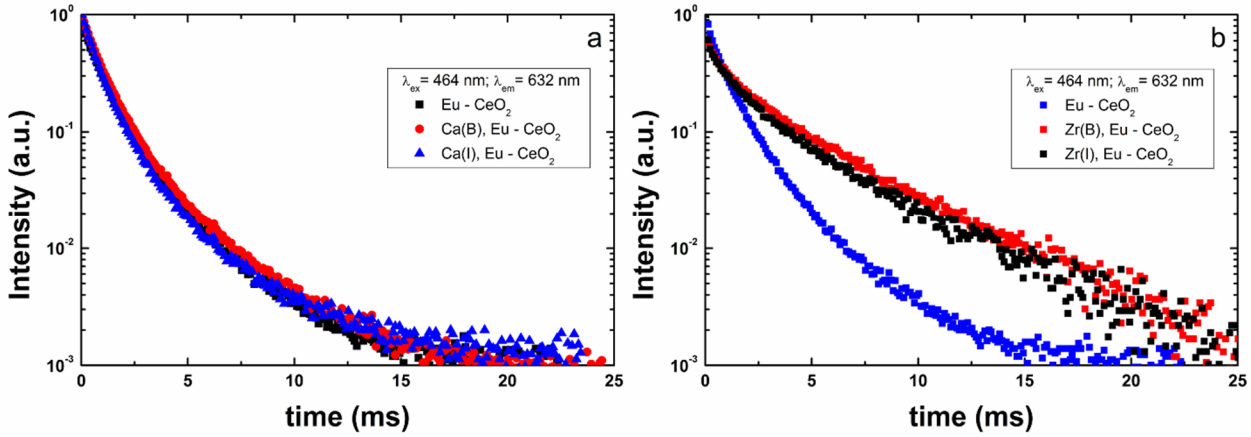

Figure S9. Emission decays of Eu- defect associate in Ca and Zr impregnated and bulked doped Eu-CeO_2 as well as Eu-CeO_2 reference sample. The comparison shows two features: (i) the Eu emission dynamics is unperturbed irrespective of Ca or Zr insertion mode and (ii) the Eu emission dynamics is strongly selective according the metal type in line with the emission spectra illustrated in **Figure 5a,c**. However, an unexpected decay lengthening compared to Eu-CeO_2 reference sample is also observed, which remains to be clarified.

Table S2. Average lifetimes of Eu emission in Ca and Zr impregnated and bulked doped CeO_2

Sample	Average lifetime of the Eu isolated center (λ_{ex}= 350 nm; λ_{em}= 591 nm) (±0.03 ms)	Average lifetime of Eu- defect associate center (λ_{ex}= 464 nm; λ_{em}= 632 nm) (±0.03 ms)
Eu-CeO_2	0.99 ms	0.94 ms
Ca(I), Eu-CeO_2	2.92 ms	0.93 ms
Ca(B), Eu-CeO_2	3.16 ms	1.06 ms
Zr(I), Eu-CeO_2	2.85 ms	1.34 ms
Zr(B), Eu-CeO_2	3.12 ms	1.41 ms

References

S1. M. Lungu, C. Dobrea, T. Craciunescu, I. Tiseanu, C. Porosnicu, I. Jepu and I. Mustata, *Digest Journal of Nanomaterials and Biostructures*, 2014, **9**, 899-906.

S2. C. Tiseanu, V. Parvulescu, M. Boutonnet, B. Cojocaru, P. Primus, C. Teodorescu, C. Solans and M. Dominguez, *Physical Chemistry Chemical Physics*, 2011, **13**, 17135-17145.

S3. M. ROMEO, K. BAK, J. ELFALLAH, F. LENORMAND and L. HILAIRE, *Surface and Interface Analysis*, 1993, **20**, 508-512.

S4. P. Burroughs, A. Hamnett, A. F. Orchard and G. Thornton, *Journal of the Chemical Society, Dalton Transactions*, 1976, **17**.

S5. X. Li, R. Wang, F. Zhang and D. Zhao, *Nano Letters*, 2014, **14**, 3634-3639.